

Article

# Geochemical Anomalies of Frozen Ground due to Hydrocarbon Migration in West Siberian Cryolithozone

Anna Kurchatova <sup>1,2,\*</sup>, Victor Rogov <sup>1,3,4</sup> and Natalia Taratunina <sup>5</sup><sup>1</sup> Institute of the Earth Cryosphere Tyum NC SB RAS, 625000 Tyumen, Russia; rogovvic@mail.ru<sup>2</sup> Tyumen Industrial University, 38 st. Volodarskogo, 625000 Tyumen, Russia<sup>3</sup> Faculty of Geography, Lomonosov Moscow State University, Leninskiye Gory, 1, 119991 Moscow, Russia<sup>4</sup> Tyumen State University, 6 st. Volodarskogo, 625003 Tyumen, Russia<sup>5</sup> Skolkovo Institute of Science and Technology, 3 st. Nobelya, 121205 Moscow, Russia;

taratuninana@gmail.com

\* Correspondence: kanni@mail.ru; Tel.: +7-345-268-87-89

Received: 30 September 2018; Accepted: 19 November 2018; Published: 22 November 2018



**Abstract:** According to the study of frozen deposits in the territory south of the Taz Peninsula, geochemical processes are considered under the hydrocarbon migration from the lower productive complex. An analysis of the cryolithological structure of the frozen stratum was performed, and the composition of the gas and authigenic associations was studied. It was shown that the migration of gases is caused by shear deformations with the formation of cryogenic textures with the presence of gas-bearing ice crystallites on slip surfaces. It was found that the migration of hydrocarbons causes significant local changes in pH/Eh parameters in the frozen stratum and determines the micromosaic distribution of sulfate and iron reduction processes that lead to the formation (including microbiological processes) of various forms of iron: sulphides, carbonates and oxides.

**Keywords:** cryolithozone; hydrocarbon migration; hydrolaccolith; authigenic minerals; biomorphic structures

## 1. Introduction

The problem of the emission of carbon dioxide and methane from the frozen stratum has been one of the most acute and controversial topics since the end of the last century, when the effect of the emission on the rise in the temperature of the atmosphere at high latitudes was shown. Most of these studies are devoted to the calculation of organic carbon stocks buried in syncrigenic rocks [1]. However, the question of the velocity of the microbial decomposition of organic matter and the emission of greenhouse gases remains unclear [2]. At the same time, direct migration of deep hydrocarbon fluids through the frozen thickness was established by geochemical and geophysical methods. Thus, geochemical studies of gas content (C<sub>1</sub>–C<sub>6</sub>, H<sub>2</sub>, CO<sub>2</sub>, N<sub>2</sub>) in snow and sediments are used to search for promising areas of hydrocarbon deposits in West Siberia. Nevertheless, this important natural factor has not received attention in the studies of the Arctic and sub-Arctic territories. Permafrost is still perceived as an impenetrable screen for gases [3,4] with a low activity of biochemical processes [5]. However, geochemical studies outside the permafrost zone established that prolonged migration of hydrocarbons and the macro- and micro-penetration of gases led to the formation of near-surface oxidation–reduction zones, which are favorable for the life of bacteria [6]. Bacterial oxidation of light hydrocarbons can directly or indirectly lead to significant changes in pH and Eh in the sedimentary stratum, thereby changing the formation and stability zones of the various minerals that are present in the rock. The main chemical and mineralogical changes in frozen grounds caused by the migration of hydrocarbon fluids are considered in this article.

## 2. Field Region and Methods of Research

Studies of gas emission and its effects on frozen grounds were carried out on the Pestsovoye field located in the northern part of the West Siberian oil and gas basin (Nadum-Pur region of the Taz Peninsula) to the west of the giant North-Urengoy gas field (Figure 1). The Pestsovoye field also contains a large gas pool in the Cenomanian complex, but Neocomian gas constitutes the principal reservoir. The gas is wet and contains significant volumes of condensate. The lower productive complexes have oil fringes. To compare the molecular and isotopic compositions of gases in the reservoirs, Neocomian and Jurassic gases are typically thermogenic; they are isotopically much heavier ( $-38\text{‰}$  to  $-42\text{‰}$ ), contain a large fraction of ethane and heavier gases, and are moderately rich in condensate (Tables 1 and 2). Gases tested from Jurassic rocks in several fields of the Nadum-Pur region have similar characteristics. In spite of the large compositional difference between Cenomanian and Neocomian gases, the concept of different sources for these gases is problematic. Geologic considerations indicate that vertical migration of hydrocarbons in the northern West Siberian basin is feasible [7].

**Table 1.** Isotopic composition of natural gases north of the Western Siberia Nadym-Pur region, the Taz peninsula [8].

Fields	Phase	$T_{ph}$ , °C	Depth, m	C2–C4, %	$d^{13}C_{CH_4}$ , ‰	$dD_{CH_4}$ , ‰
Cenomanian Complex						
Noth-Urengoy, Pestsovoye	Gas	30–37	1043–1350	0–0.56	–50.86– –56.11	–204.5– –218.7
Lower Cretaceous Complex						
Pestsovoye	Oil–gas– condensate	62.5–93	1836–3380	1.32–12.16	–38.00– –41.31	–207.2– –230.7
Noth-Urengoy	Gas–condensate, oil–gas–condensate	66.0–82.6	2546–3180	1.39–15.4	–35.09– –38.78	–226.8– –237.5
Jurassic Complex						
Etypurskoe (J <sub>3</sub> )	Oil–gas–condensate	83–101	2907–3058	10.50–26.10	–40.70– –42.88	–257.7– –258.0
Pestsovoye (J <sub>3</sub> , J <sub>2</sub> )	Oil–gas–condensate	112	3800–4000	16.5–17.5		

$T_{ph}$ —Temperature of the phase, °C;  $d^{13}C_{CH_4}$ —The ratio of carbon isotopes for methane in different fields, ‰;  $dD_{CH_4}$ —The ratio of hydrogen isotopes for methane in different fields, ‰; J—Jurassic deposits.

**Table 2.** Isotope composition of methane carbon from Cenomanian gas pools [8].

Fields	Well	Depth, m	Gas Composition, %									$d^{13}C_{CH_4}$ , ‰
			CH <sub>4</sub>	C <sub>2</sub> H <sub>6</sub>	C <sub>3</sub> H <sub>8</sub>	C <sub>4</sub> H <sub>10</sub>	CO <sub>2</sub>	N <sub>2</sub>	He	Ar	H <sub>2</sub>	
Noth-Urengoy	74	1208–1212	99.20	0.004	0.001	-	-	0.80	0.014	0.007	0.001	–53.56
Pestsovoye	3	1260–1268	98.10	0.340	0.160	0.054	0.09	1.23	0.017	0.010	-	–52.63

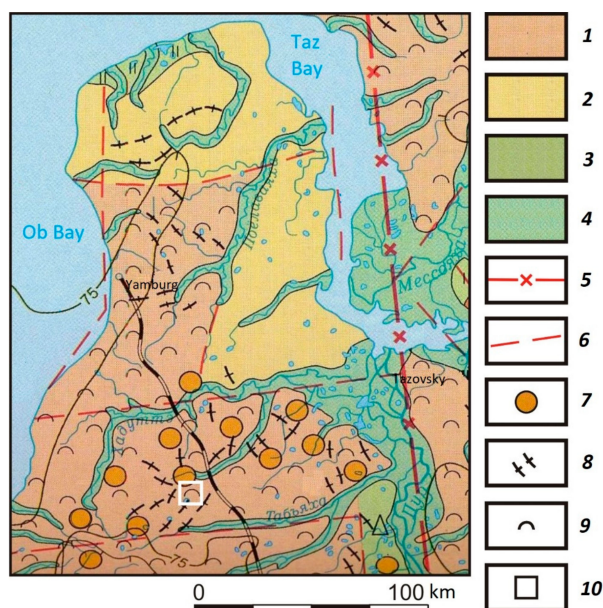


**Figure 1.** Location of the research area [9]. 1—elevations and ridges 80–100 m; 2—plains 30–60 (80) m; 3—lowlands and plains 0–25 (30) m; 4—river valleys; 5—regional fracture; 6—lineaments; 7—uplift of Paleogene clay expressed in relief; 8—parallel ridge relief; 9—hydrolaccolith; 10—research area.

The field is located in the zone of continuous permafrost development. The existence of melt zones was established under the riverbeds and lakes. The thickness of frozen stratum ranges from 300 m to 450 m for the main part of the territory, and 50 m to 150 m for river valleys. The territory is characterized by a wide distribution of the frost mounds with an ice core (hydrolaccolith) [10]. The formation of a hydrolaccolith is associated with the dislocations of the Paleogene diatomite bed; the structural uplifts are caused largely by the inversion of the rock density along the section [11] since the bulk density of Paleogene diatomites ( $0.8\text{--}1.0\text{ g/cm}^3$ ) is much smaller than the overlapping Oligocene–Quaternary sandy–loamy deposits ( $1.8\text{--}2.0\text{ g/cm}^3$ ). In the upper part of the section, diatom clays are characterized by high ice content exceeding the total moisture capacity of the rocks; salinity is about 0.6% (up to 1.6%) mainly due to sulfates (up to 90% from the total sum of anions) [12,13].

The authors studied samples from a 35 m core obtained by drilling from the top of one of the hydrolaccoliths. Samples of frozen ground and ice were collected in winter and stored at minus  $15\text{ }^\circ\text{C}$ . Samples were prepared by the replica technique that enables the high magnification study of textural characteristics and surface features of clays and involves minimal disturbance to their morphology by the formation of a thin plastic film on the soil surface [14]. The authors have modified the replica technique to investigate the frozen ground in the scanning electron microscope: the shape, size, surface of mineral grains and soil aggregates in the initial undisturbed state were analyzed [15]. The replica method was also used to study authigenic minerals and metastable colloids in the pore space of soils and ground ice. To obtain the information about the structure of the inclusions of ice (determination of crystal sizes, orientation of their optical axes), sample preparation was supplemented by etching [16].

Determination of the composition of authigenic minerals in replicas was carried out in the Earth Cryosphere Institute, Tyumen Scientific Center of the SB RAS (Siberian Branch of the Russian Academy of Sciences) (using a scanning electron microscope TM3000 (Hitachi, Tokyo, Japan) with an Energy Dispersive X-ray Spectrometer SwiftED3000 (OXFORD Instruments, Abingdon, UK). Determination of the particle size distribution of the deposits was performed on a laser analyzer Mastersizer 3000 (Malvern Panalytical, Malvern, UK) with dispersion in an aqueous medium. Mineralogical composition of sediments, including analysis of coarse silt and fine sand fractions to determine the coefficient of cryogenic contrast (CCC), was performed using the X-ray diffractometer D2 PHASER (Bruker, Karlsruhe, Germany) by the Rietveld method. CCC was calculated from the ratio of quartz to the

sum of feldspars in fractions of 20–50  $\mu\text{m}$  and 50–100  $\mu\text{m}$ , respectively [16]. The analysis of the gas composition of ice and ground samples was carried out using a gas chromatograph 1D-GC with a flame ionization detector in the Laboratory of Oil and Gas Geochemistry at the Tyumen Industrial University. The detector was calibrated to determine the microconcentrations of hydrocarbon gases. The detection limit was set to  $1 \times 10^{-6}$  vol. % [17].

### 3. Results

Deposits underlying the ice core of the frost mound were exposed by drilling (ice was found at a depth of 13–26.5 m from the hydrolaccolith summit), which are represented by diatom clays with inclusions of interlayers of more sandy material. Mineral grains are clearly divided into angular quartz particles and weathered silicates; accessory minerals are ilmenite, rutile and zircon. A characteristic feature of the sediments is the absence of colloid films on the mineral grains and diatoms.

Two systems of cryotexture were identified in the diatom clay (Figure 2). The first order consists of the sub-horizontal ice layers up to the first centimeter thick; the second order forms oblique parallel layers (up to 250  $\mu\text{m}$ ) in compacted clay. Ice layers are composed of plane-faced isometric crystals. The orientation of their main optical axes is transverse, which is characteristic for segregated ice lenses [16]. In separate layers, there are both isometric and elongated crystals, as well as dense clay aggregates. The ice layers have vertical displacements, zigzag bends with the twinning of crystals at nodes.

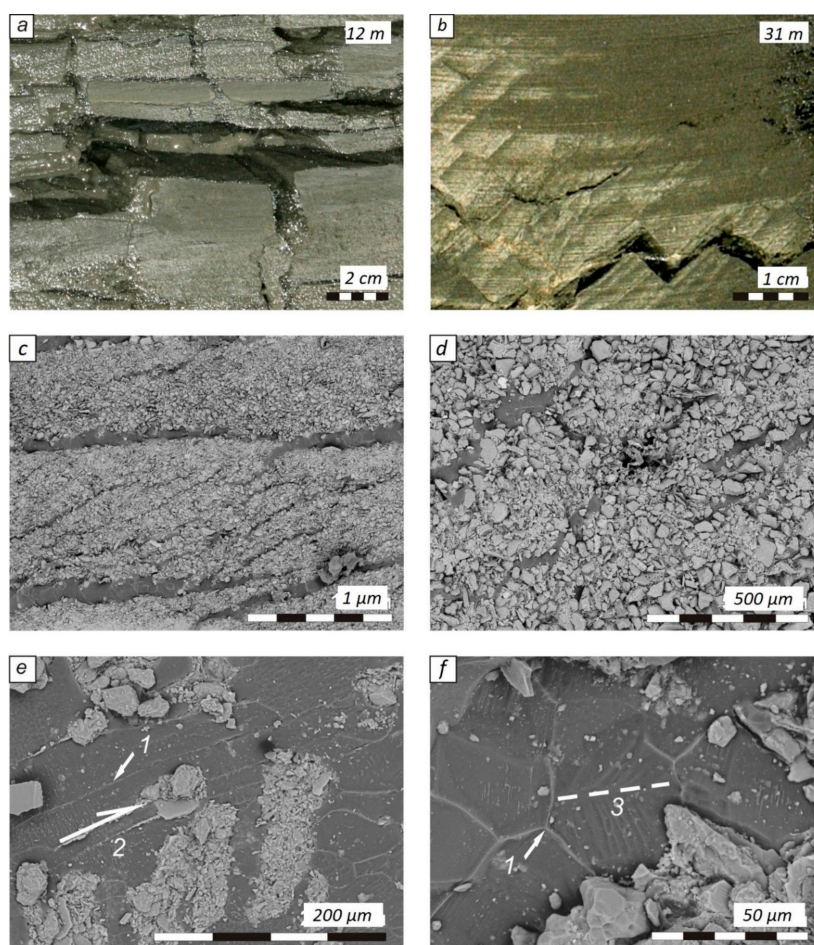


**Figure 2.** Cryogenic texture. (a) Reticulated cryotexture of sediments over the ice core; (b) cracked cryotexture of sediments, underlying the ice core; (c) horizontal and inclined systems of ice lenses; (d) displacements of ice layers; (e) shear deformation in the ice layer; (f) twinning of a crystal on the bend of an ice lens; 1—Boundary of ice crystals; 2—Shear direction; 3—Crystal twinning axis.

Methane concentration in the samples of diatom clays is 7.6 vol. % and 2.2 vol. % in the ground and in ice, respectively (Figure 3a,b). Homologs of methane  $C_2$ – $C_4$  are the most useful gases to determine the vertical migration of hydrocarbons in geochemical petroleum surveys because they are not produced by biological processes in near surface sediments and therefore provide the most sensitive indicators of deep-source reservoir fluids [18]. Typical background ambient air ethane concentrations are generally less than 2 ppb. According to a surface geochemical survey in the Nadum-Pur region, the background values of the sum of methane homologs are about 0.00007 grams per ton. Values more than 0.0025 g/t often correlate with aquifers [17]. The highest methane concentration correlates well with the sum of light hydrocarbons and is observed at the base of the hydrolaccolith below the ice core.

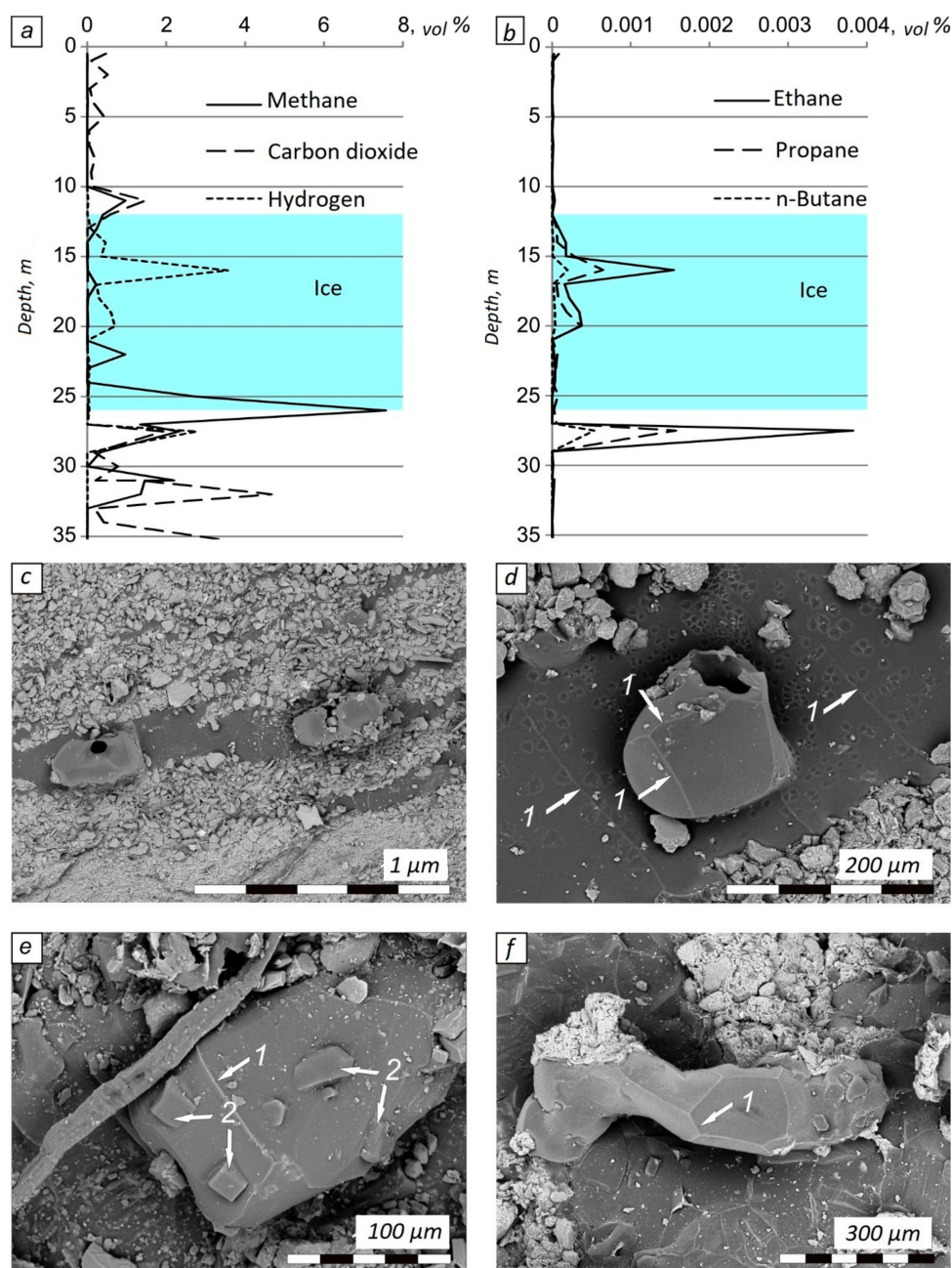


**Figure 3.** Gas concentration along the section (a,b) and gas inclusions in sediments of hydrolaccolith (c) spherical crystallites in the ice layer; (d) destroyed crystallite; (e) box shape of crystallite; (f) elongated form of crystallite); 1—Boundaries of ice crystals; 2—Etching figures.

Areas of high concentration of carbon dioxide and excessive hydrogen content refer to indirect signs of oil and gas occurrence, since they relate to products of secondary conversion of hydrocarbons under the influence of microbiological, oxidative and other processes [19]. A significant number of gas bubbles are established in the samples of frozen ground and ice; they form extended chains along the deformation cracks. Together with gas bubbles, hollow, curved spherical and elongated formations are found in the ice layers of diatom clay (Figure 3c–f); the hexagonal faces and etching patterns on them indicate the crystalline structure of ice. Such anomalous crystals with gas inclusions can grow in heterophase fluid in the presence of salt melt-brine and gas bubbles which is typical for fluid-saturated residual melts [20]. Gas-bearing crystallites are generally formed along the growth zones and crystal faces or tend to occur solitary or isolated [21] while gas bubbles are trapped in the fractures. These inclusions occur as trails or clusters which often cut across the grain boundaries.

Various generations of sulfides were found in clay samples at the base of the frost mound below the ice core at depths of 30–35 m: amorphous hydrotroilite framboids, marcasite aggregates and pyrite crystals (Figure 4a–d). There are newly formed carbonates (siderite) and magnetite (Figure 4e,f, respectively) in some samples, which are usually formed at the periphery of gas and oil fields.

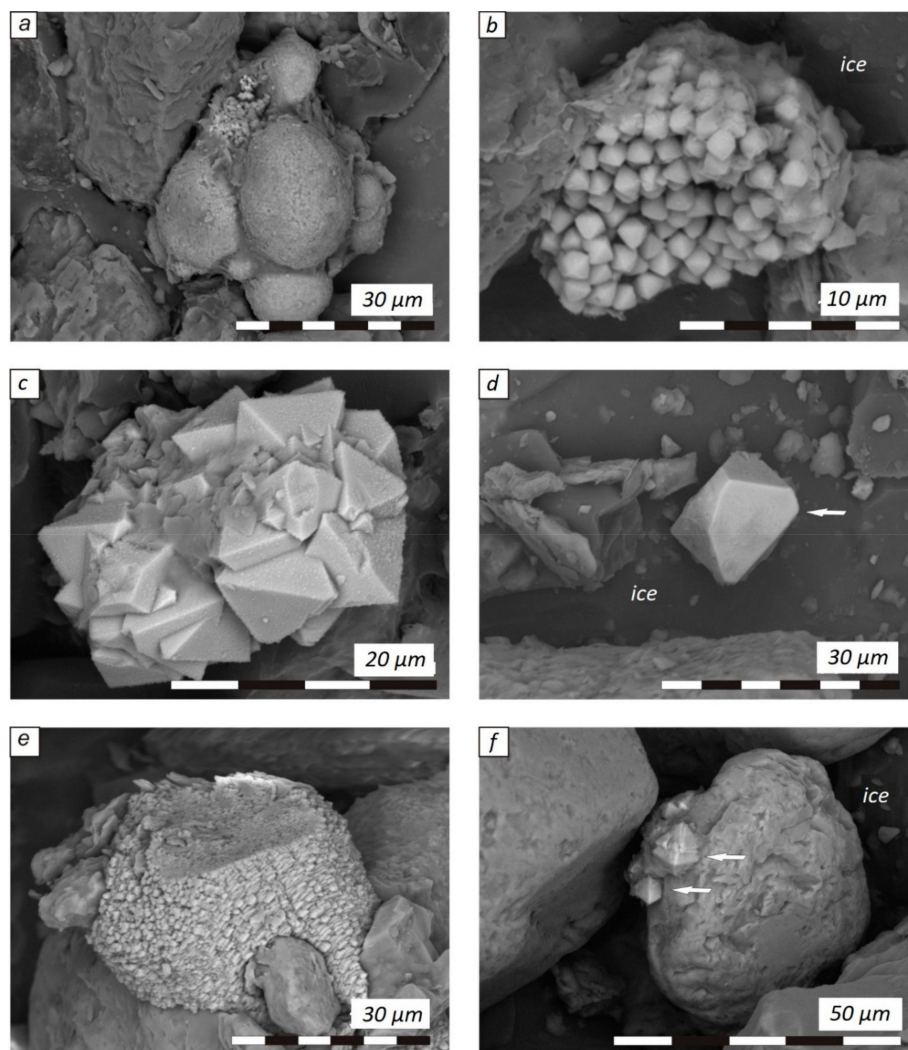


**Figure 4.** Authigenic minerals. (a) Colloidal aggregate of iron sulfide; (b) framboid of pyrite crystals; (c) marcasite joint, (d) pyrite; (e) colloidal aggregate of siderite; (f) magnetite.

#### 4. Discussion

The results of the surface geochemical survey in West Siberia show the widespread occurrence of hydrocarbon migration as the reservoir leaks through permafrost strata [17]. The pressure drop upwards from the reservoir determines the possibility of forming filtration (microfiltration) processes through a system of open pores and cracks formed on the arches of growing uplifts [22]. In permafrost (taking into account the rheological properties of frozen grounds), it can be provided by fracture permeability. With prolonged shear deformations, the dislocations develop in the ground along the weakness zones—gas inclusions in the pore space following discharge of water on slip planes and the formation of parallel inclined ice layers. Numerous examples of cryogenically destroyed mineral grains of quartz and brittle structures of feldspars were found in these zones (Figure 5) [16,23]. The CCC values of 0.94, 1.16, 1.29 and 0.96 at a depth of 31 m, 32 m, 33 m and 34 m, respectively, confirm the cryogenic mechanism of sediment destruction, which is probably due to multiple phase transitions as a result of localization of the pore water in the shear zone. Below this, at a depth of 35.5 m, the CCC is 0.70, which reflects the conditions of humid lithogenesis without significant influence of water–ice phase transitions [24].

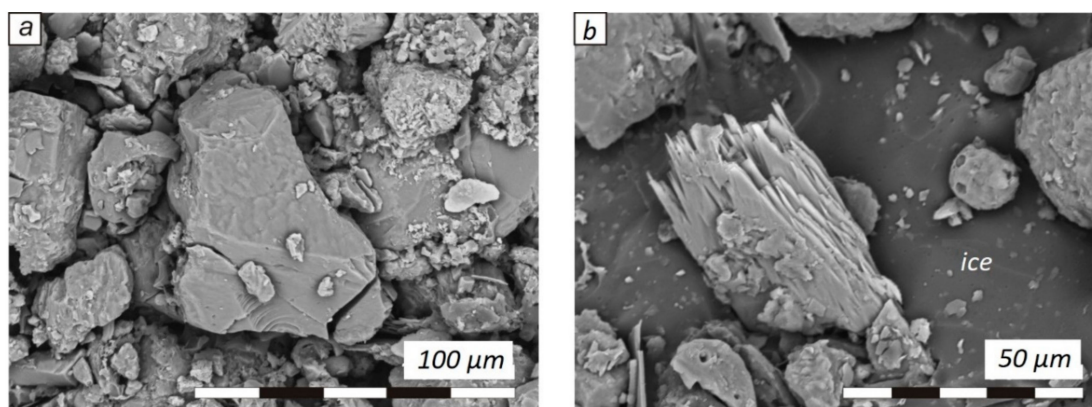
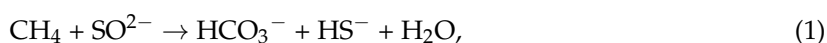


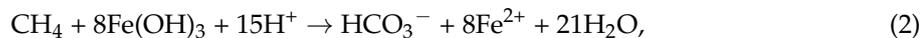
**Figure 5.** Cryogenic destruction of mineral grains. (a) Quartz; (b) feldspar.

On the whole, a pronounced reduction medium with a predominance of hydrogen ions and a high content of ferrous iron is characterized for the frozen stratum [16], where complexes of authigenic iron sulfides are characteristic for certain facial conditions (for example, alas deposits). However, the mineral series of newly formed sulfides in diatomaceous clays at the base of the hydrolaccolith (hydrotroilite, marcasite, pyrite) corresponds more to the associations of authigenic minerals of reservoir rocks and hydrate-saturated marine sediments [25] than syncriogenic lake sediments represented by sooty concretions of melnikovite ( $\text{FeS Fe}_2\text{S (Fe}_3\text{S}_4)$ ), greigite ( $\text{Fe}_3\text{S}_4$ ) or mackinavite ( $\text{Fe}_9\text{S}_8$ ) [26]. It should be noted that a similar regime of formation of authigenic sulfides in the various environmental conditions occurs primarily due to multiple phase transitions of water during the freezing of sediments.

Amorphous hydrotroilite framboids with a high iron content, established in samples from a depth of 29–34 m (Figure 6a,b), are morphologically similar to biomorphic structures found in natural anaerobic methane environments, regardless of the temperature of the medium, depth, pressure, or methane concentration [27–29]. Thus, bacterial conglomerates of uncultivated archaea, close to *Methanosarcinales* and *Methanobacteriales*, and sulfate reducers, probably related to *Desulfosarcina/Desulfococcus*, were established in the hydrate-saturated sediments of methane seeps by a fluorescent method. It is assumed that methanogenic archaea oxidize methane and form hydrogen through a reverse reaction to the reduction of  $\text{CO}_2$ ; in turn, sulfate-reducing microorganisms actively consume hydrogen and control its low concentration [30,31]:



In sulfate-depleted anaerobic ecosystems of freshwater and brackish sediments, methane oxidation can occur due to microbial iron reduction, since oxidized solid phases such as iron oxides are also thermodynamically advantageous electron acceptors (Fe-AOM) [32]:



As a result of microbial iron reduction, authigenic minerals are formed: in particular, magnetite and siderite [33,34]. Thus, in the studied samples from the core of the hydrolaccolith in the clay pore space, iron sulfides are most often found, and in sandy interlayers, predominantly granular siderite aggregates located on the surface of the mineral grains (or cementing them) were found. Apart from authigenic siderite, clusters globules of Fe-carbonate were found in the sample from a depth of 29 m (Figure 6c,d); similar nanostructures could be formed by bacteria *Acidiphilium* sp. in a weakly acidic (pH = 5–7) reducing (Eh < 0) medium [35].

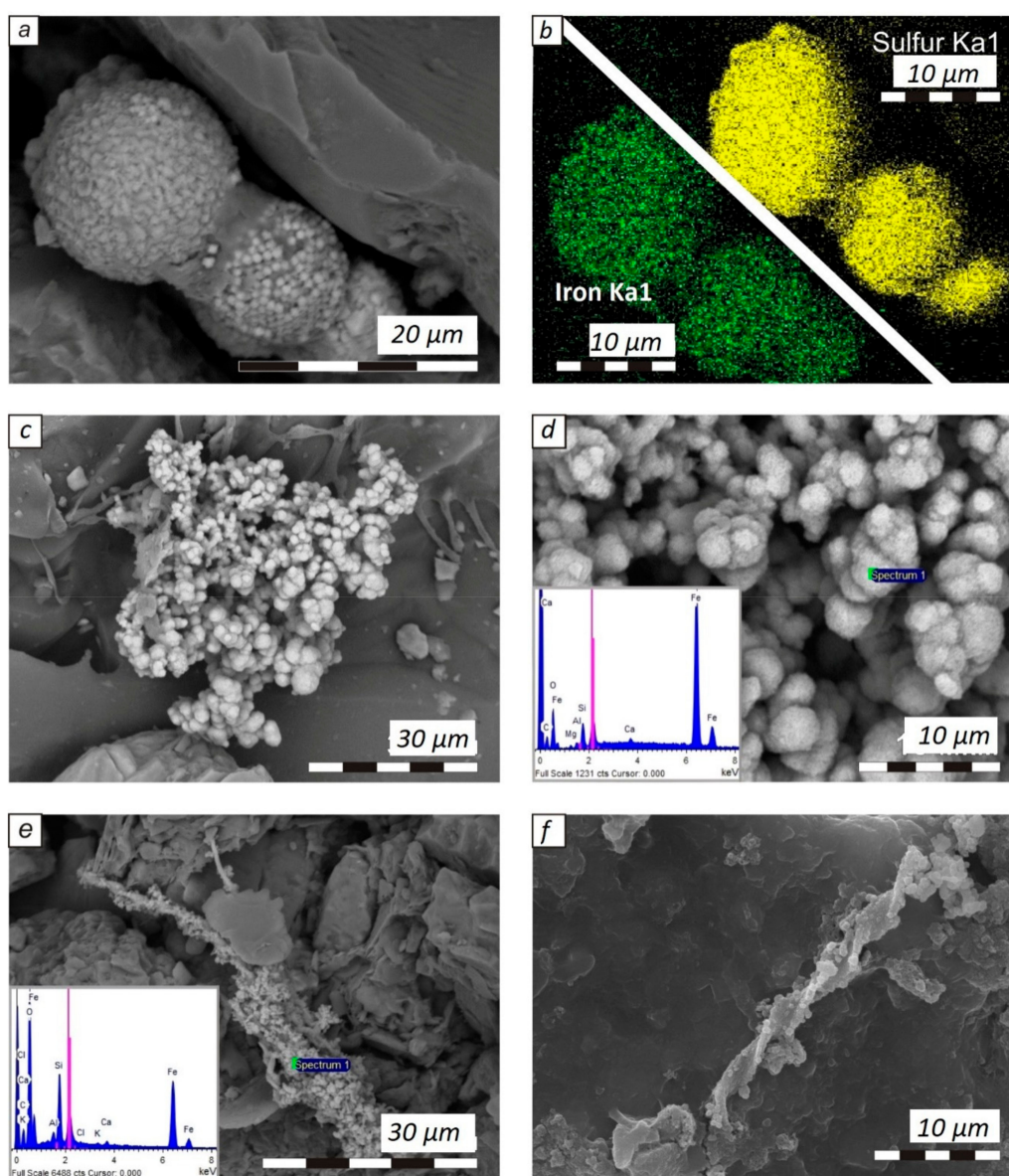


**Figure 6.** Biomorphic structures. (a) Colloidal aggregate of iron sulfide; (b) spectral microanalysis: maps of distribution of iron (green) and sulfur (yellow); (c) siderite nanoglobules; (d) spectral microanalysis of siderite nanoglobules; (e) iron-containing structure and its spectral microanalysis; (f) iron-containing structure with elements of a double helix, like bacteria fibrils *Galionella*.

The second type of iron-containing structures are morphologically similar to curved spirals formed by *Gallionella* iron bacteria (Figure 6e,f), which live in an environment close to neutral under aerial and microaerophilic conditions [36]. The local emergence of oxygen in the anaerobic atmosphere of frozen stratum is possible under the crystallization of supercooled pore water in the slip zone. Indirectly, active iron reduction is evidenced by the absence of colloidal films on the surface of mineral grains and diatoms; the latter, therefore, are easily determined by microscopic studies even without special sample preparation.

It should be noted the feature of the micromosaic distribution of sites with different pH/Eh conditions, which controls the new formation of iron in the form of siderite, sulfides or oxide, is observed by micro-interlayers of sand and clay. An example of such a natural system in which dissolved carbonate and sulfur can simultaneously take part are sedimentary iron ores [37]. For such systems, Garrels and Krayst [38] give a combined Eh/pH diagram (Figure 7a), an analysis of which shows that siderite has a significant stability only under conditions of high activity of dissolved carbonate (as is typical for supercooled pore waters) and extremely low activity reduced sulfur for equilibrium ratios at  $\Sigma\text{CO}_2 = 10^0$  and  $\Sigma\text{S} = 10^{-6}$ . At the same time, the authors [38] emphasize that at low temperatures, the sulfate ion will be restored extremely slowly, unless living organisms participate in this process. The detection in the sample from a depth of 34 m of sulfur nanoglobules (Figure 7b) shows the possibility of the participation of bacteria of the family *Ectothiorhodospiraceae*, which are capable of forming elemental sulfur globules outside their cells [39] in authigenic mineral formation in the zone of fluid permeability of frozen stratum.

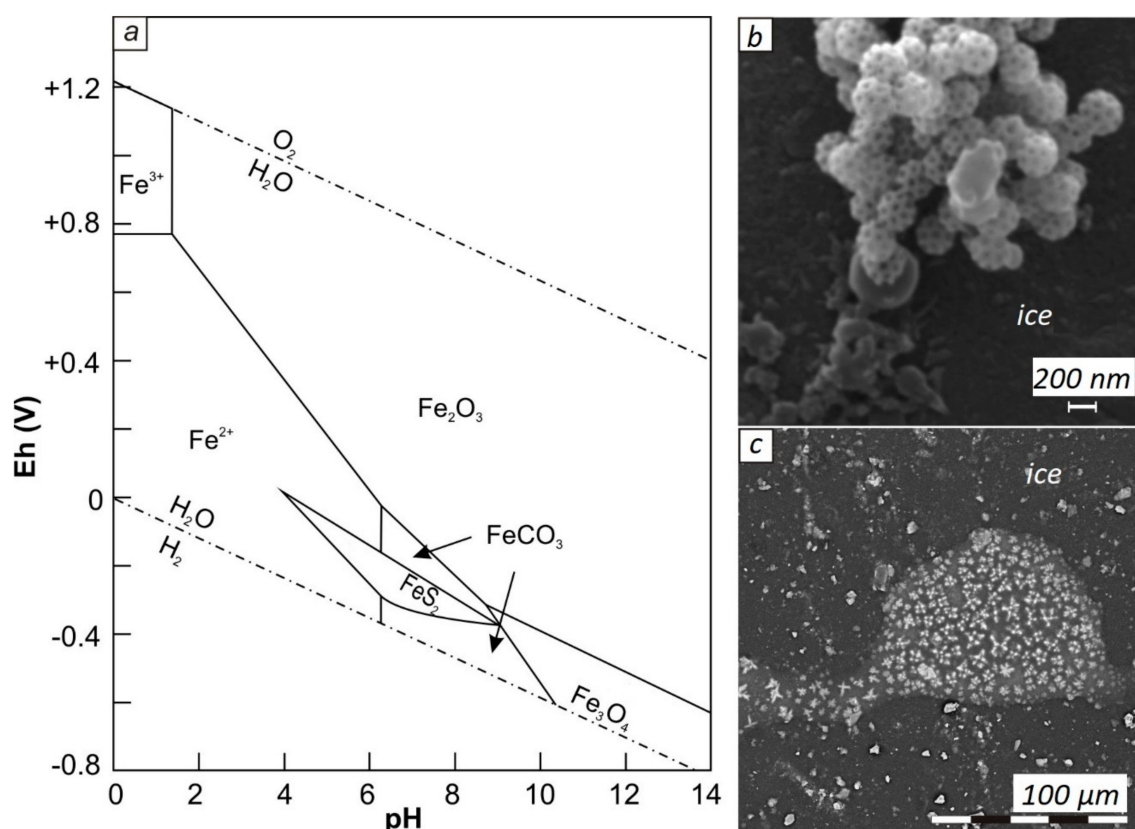


**Figure 7.** Geochemical conditions of stability of iron minerals in solutions. (a) Combined Eh–pH diagram of equilibrium ratio of oxides, sulfides and iron carbonate in water at 25 °C and 1 atm. ( $\Sigma\text{CO}_2 = 10^0$  and  $\Sigma\text{S} = 10^{-6}$ ) [33]; (b) sulfur nanoglobules in the sample, h = 29 m (pH < 7); (c) lenses of chlorides in ice in the same sample (pH > 7).

The recovery condition caused by the migration of hydrocarbons, first of all methane, with enough ferric iron (to maintain low concentrations of  $\text{HS}^-$ ) promotes the formation of other minerals such as magnetic oxides maghemite ( $\gamma\text{-Fe}_2\text{O}_3$ ) and magnetite ( $\text{Fe}_3\text{O}_4$ ). Such processes lead to the formation of magnetic surface anomalies over oil and gas fields. Magnetite crystallization in abiogenic medium requires high temperature and pressure, while transformation of poorly crystallized iron oxide to magnetite under anaerobic conditions and alkaline medium requires bacteria of the genus *Geobacter* [40,41]. The appearance of such local areas with high alkalinity in the studied section is possible as a result of the cryogenic concentration of chlorides during the freezing of desalinated marine deposits (Figure 7c).

## 5. Conclusions

1. Gaseous hydrocarbon migration through the frozen stratum is caused by shear deformations in permeability zones with the formation of cryogenic textures of fracture type along slip surfaces that are characterized by the presence of gas-bearing ice crystallites and high fracturing of quartz.

2. Long-term migration of hydrocarbons, especially methane, in frozen stratum causes significant changes in pH/Eh parameters: predominantly strictly anaerobic conditions can locally change to microaerophilic due to the release of oxygen during the crystallization of water in the slip zone; predominantly neutral–weakly acidic conditions can locally change to alkaline as a result of the cryogenic concentration of chlorides during the freezing of marine sediments.

3. The impulsive nature of the migration of hydrocarbons in the permeability zones of frozen stratum determines the zoning of sulfate and iron reduction processes, which determines the micromosaic distribution of new various forms of iron: sulfides, carbonates and oxides, including biogenic ones.

**Author Contributions:** A.K. and V.R. were responsible for conceptualization and methodology of this research. They conceived and planned the experiments and all authors conducted it. All authors validated the results, discussed it and contributed to the final version of the manuscript. Software, resources were provided by A.K.; data curation and writing—original draft preparation were done by V.R. Writing—review and editing, project administration were done by N.T.

**Funding:** This study was supported by Russian Science Foundation, Grant No 14–17–00131.

**Acknowledgments:** The authors would like to thank the reviewers for their valuable comments on the manuscript.

**Conflicts of Interest:** The authors declare no conflict of interest. The funders had no role in the design of the study; in the collection, analyses, or interpretation of data; in the writing of the manuscript, or in the decision to publish the results.

## References

1. Bischoff, J.; Mangelsdorf, K.; Gattinger, A.; Schloter, M.; Kurchatova, A.N.; Herzsuh, U.; Wagner, D. Response of methanogenic archaea to Late Pleistocene and Holocene climate changes in the Siberian Arctic. *Glob. Biogeochem. Cycles* **2013**, *27*, 305–317. [[CrossRef](#)]
2. Schuur, E.A.G.; McGuire, A.D.; Schaedel, C.; Grosse, G.; Harden, J.W.; Hayes, D.J.; Hugelius, G.; Koven, C.D.; Kuhry, P.; Lawrence, D.M.; et al. Climate change and the permafrost carbon feedback. *Nature* **2015**, *520*, 171–179. [[CrossRef](#)] [[PubMed](#)]
3. Hubberten, H.W.; Romanovskii, N.N. The main features of permafrost in the Laptev Sea region, Russia—A review. In Proceedings of the 8th International Conference on Permafrost, Zürich, Switzerland, 21–25 July 2003; pp. 431–436.
4. Leibman, M.O.; Perednya, D.D.; Kizyakov, A.I.; Lein, A.Y.; Savvichev, A.S.; Vanshtein, B.G. Sulfur and carbon isotopes within atmospheric, surface and ground water, snow and ice as indicators of the origin of tabular ground ice in the Russian Arctic. *Permafrost Periglacial Process.* **2011**, *22*, 39–48. [[CrossRef](#)]
5. Yergeau, E.; Hogues, H.; Whyte, L.G.; Greer, C.W. The functional potential of high Arctic permafrost revealed by metagenomic sequencing, qPCR and microarray analyses. *ISME J.* **2010**, *4*, 1206–1214. [[CrossRef](#)] [[PubMed](#)]
6. Schumacher, D. Hydrocarbon-induced alteration of soils and sediments. *AAPG MEMOIRS* **1996**, *66*, 71–89.

7. Smith-Rouch, L.S. Petroleum Geology and Resources of the West Siberian Basin, Russia. *US Geol. Surv. Bull.* **2006**, *27*, 2201.
8. Schoell, M.; Picha, F.; Rovenskaya, A.; Nemchenko, N. Genetic characterization of natural gases in NW Siberia. In Proceedings of the American Association of Petroleum Geologists International Conference, Vienna, Austria, 7–10 September 1997; pp. 46–47.
9. The newest tectonics of flat territory (with elements of structural geomorphology). In *Atlas of the Yamal-Nenets Autonomous District*; FGUP Omskaya kartograficheskaya fabrika: Omsk, Russia, 2004; pp. 60–61. (In Russian)
10. Vasil'chuk, Yu.K.; Budantseva, N.A.; Vasil'chuk, A.C.; Yoshikava, I.; Podborny, Ye.Ye; Chizhova, Ju.N. Isotopic composition of the ice core of the Late Pleistocene bulgunyah at the Pestsovoye deposit in the Evoya River valley in the south of the Taz Peninsula. *Kryosfera Zemli* **2014**, *18*, 47–58. (In Russian)
11. Kuzin, I.L. *Geomorphology of the West Siberian Plain*; State. Polar. Academy: Sankt-Peterburg, Russia, 2005; p. 176. (In Russian)
12. Dubikov, G.I. Composition and Cryogenic Structure of the Frozen Strata of Western Siberia. GEOS: Moscow, Russia, 2002; p.246. (In Russian)
13. Kritsuk, L.N. *Underground Ice Cryolithozone of Western Siberia*; Scientific World: Moscow, Russia, 2010; p. 350. (In Russian)
14. Bates, T.F.; Comer, J.J. Electron microscopy of clay surfaces. *Clays Clay Miner.* **1955**, *3*, 1–25. [[CrossRef](#)]
15. Rogov, V.V.; Kurchatova, A.N. Method of Manufacturing Replica for Analyses of Microstructure of Frozen Rocks in Scanning Electron Microscope. RU Patent 2,528,256 C1, 2013. Available online: <http://russianpatents.com> (accessed on 13 January 2013).
16. Rogov, V.V. *Fundamentals of Cryogenesis*; GEO: Novosibirsk, Russia, 2009; p. 202. (In Russian)
17. Zavatskiy, M.D. Study of the Fields of Hydrocarbon Gas Concentrations in Surface Natural Sorbents in Connection with Prospecting and Exploration of Oil and Gas Deposits in Western Siberia. Ph.D. Thesis, TSOGU, Tyumen, Russia, 2009. (In Russian)
18. Jones, V.T.; Drozd, R.J. Predictions of oil or gas potential by near surface geochemistry. *Am. Assoc. Pet. Geol. Bull.* **1983**, *67*, 932–952.
19. Milkov, A.V. Worldwide distribution and significance of secondary microbial methane formed during petroleum biodegradation in conventional reservoirs. *Org. Geochem.* **2011**, *42*, 184–207. [[CrossRef](#)]
20. Randive, K.R.; Hari, K.R.; Dora, M.L.; Malpe, D.B.; Bhondwe, A.A. Study of Fluid Inclusions: Methods, Techniques and Applications. *Geol. Mag.* **2014**, *29*, 19–28.
21. Kurchatova, A.N.; Mel'nikov, V.P.; Rogov, V.V. Gas-bearing ice crystallites in clayey deposits. *Dokl. Earth Sci.* **2014**, *459*, 1510–1513. [[CrossRef](#)]
22. Gogonenkov, G.; Timurziev, A. Strike-slip deformations in the West Siberian basin and their impact of exploration and development of oil and gas reservoirs. *Cent. Eur. Geol.* **2009**, *52*, 359–390. [[CrossRef](#)]
23. Gibson, E.K.; Wentworth, S.J.; McKay, D.S. Chemical weathering and diagenesis of a cold desert soil from Wright Valley, Antarctica: An analog of Martian weathering processes. *J. Geophys. Res.* **1983**, *88*, 912–928. [[CrossRef](#)]
24. Konishchev, V.N.; Rogov, V.V. Investigations of cryogenic weathering of Europe and Northern Asia. *Permafrost Periglac. Process.* **1993**, *4*, 49–64. [[CrossRef](#)]
25. Kurchatova, A.N.; Slagoda, E.A.; Obzhirov, A.I.; Shakirov, R.B.; Rogov, V.V. *Microstructure of diatomaceous muds of hydrate-saturated deposits of the Okhotsk Sea/Arctic, Subarctic: Mosaic, contrast*, In *Cryosphere Variability/Abstracts of the International Conference*; Epokha: Tyumen, Russia, Russia 2015. (In Russian)
26. Kurchatova, A.N.; Rogov, V.V. Authigenic carbonates in sediments of the Ice Complex of the Coastal Plains of the Eastern Arctic. *Kriosf. Zemli. Earth's Cryosphere* **2013**, *17*, 60–69. (In Russian)
27. Hoehler, T.M.; Alperin, M.J.; Albert, D.B.; Martens, C.S. Field and laboratory studies of methane oxidation in an anoxic marine sediment: Evidence for a methanogen-sulfate reducer consortium. *Glob. Biogeochem. Cycles* **1994**, *8*, 451–463. [[CrossRef](#)]
28. Hinrichs, K.-U.; Hayes, J.M.; Sylva, S.P.; Brewer, P.G.; DeLong, R.F. Methane-consuming archaeobacteria in marine sediments. *Nature* **1999**, *398*, 802–805. [[CrossRef](#)] [[PubMed](#)]
29. Reed, D.W.; Fujita, Y.; Delwiche, M.E.; Blackwelder, D.B.; Sheridan, P.P.; Uchida, T.; Colwell, F.S. Microbial Communities from Methane Hydrate-Bearing Deep Marine Sediments in a Forearc Basin. *Appl. Environ. Microbiol.* **2002**, *68*, 3759–3770. [[CrossRef](#)] [[PubMed](#)]

30. Boetius, A.; Ravensschlag, K.; Schubert, C.J.; Rickert, D.; Widdel, F.; Gieseke, A.; Amann, R.; Jørgensen, B.B.; Witte, U.; Pfannkuche, O. A marine microbial consortium apparently mediating anaerobic oxidation of methane. *Nature* **2000**, *407*, 623–626. [[CrossRef](#)] [[PubMed](#)]
31. Knittel, K.; Lösekann, T.; Boetius, A.; Kort, R.; Amann, R. Diversity and distribution of methanotrophic archaea at cold seeps. *Appl. Environ. Microbiol.* **2005**, *71*, 467–479. [[CrossRef](#)] [[PubMed](#)]
32. Sivan, O.; Adler, M.; Pearson, A.; Gelman, F.; Bar-Or, I.; John, S.G.; Eckert, W. Geochemical evidence for iron-mediated anaerobic oxidation of methane. *Limnol. Oceanogr.* **2011**, *56*, 1536–1544. [[CrossRef](#)]
33. Egger, M.; Rasigraf, O.; Sapart, C.J.; Jilbert, T.; Jetten, M.S.M.; Röckmann, T.; van der Veen, C.; Bândă, N.; Kartal, B.; Ettwig, K.F.; et al. Iron-Mediated Anaerobic Oxidation of Methane in Brackish Coastal Sediments. *Environ. Sci. Technol.* **2015**, *49*, 277–283. [[CrossRef](#)] [[PubMed](#)]
34. Slobodkin, A.I. Thermophilic Iron-Reducing Prokaryotes. Ph.D. Thesis, Institute of Microbiology of the Russian Academy of Sciences, Moscow, Russia, 2008. (In Russian)
35. Sánchez-Román, M.; Fernández-Remolar, D.; Amils, R.; Sánchez-Navas, A.; Schmid, T.; Martin-Uriz, P.S.; Rodríguez, N.; McKenzie, J.A.; Vasconcelos, C. Microbial mediated formation of Fe-carbonate minerals under extreme acidic conditions. *Sci. Rep.* **2014**, *4*, 4767. [[CrossRef](#)] [[PubMed](#)]
36. Engel, A.S. Geomicrobiology of Sulfuric Acid Speleogenesis: Microbial Diversity, Nutrient Cycling, and Controls on Cave Formation. Master's Thesis, The University of Texas, Austin, TX, USA, 2004.
37. Eby, G.N. *Principles of Environmental Geochemistry*; Brooks/Cole: Boston, MA, USA, 2004.
38. Garrels, R.M.; Krayst, C.L. *Solutions, Minerals, Equilibrium*; Harper & Row: New York, NY, USA, 1965.
39. Imhoff, J.F. The family Ectothiorhodospiraceae. In *Prokaryotes*; Springer: New York, NY, USA, 2006; pp. 874–886.
40. Frankel, R.B.; Bazylinski, D.A. Biologically Induced Mineralization by Bacteria. *Rev. Miner. Geochem.* **2003**, *54*, 95–114. [[CrossRef](#)]
41. Weber, K.A.; Achenbach, L.A.; Coates, J.D. Microorganisms pumping iron: Anaerobic microbial iron oxidation and reduction. *Nat. Rev. Microbiol.* **2006**, *4*, 752–764. [[CrossRef](#)] [[PubMed](#)]



© 2018 by the authors. Licensee MDPI, Basel, Switzerland. This article is an open access article distributed under the terms and conditions of the Creative Commons Attribution (CC BY) license (<http://creativecommons.org/licenses/by/4.0/>).